Hindawi Publishing Corporation
Mathematical Problems in Engineering
Volume 2014, Article ID 529293, 13 pages
http://dx.doi.org/10.1155/2014/529293

*Research Article*

# Sliding Mode Control for Active Suspension System with Data Acquisition Delay

**Uiliam Nelson L. T. Alves, José Paulo F. Garcia, Marcelo C. M. Teixeira, Saulo C. Garcia, and Fernando B. Rodrigues**

*Control Research Laboratory, Department of Electrical Engineering, Univ Estadual Paulista (UNESP), Carlos Rossi, Avenue No. 1370, 15385-000 Ilha Solteira, SP, Brazil*

Correspondence should be addressed to Uiliam Nelson L. T. Alves; uiliamlendzionalves@gmail.com

Received 29 October 2013; Revised 7 February 2014; Accepted 12 February 2014; Published 9 April 2014

Academic Editor: Dan Wang



This paper addresses the problem of control of an active suspension system accomplished using a computer. Delay in the states due to the acquisition and transmission of data from sensors to the controller is taken into account. The proposed control strategy uses state predictors along with sliding mode control technique. Two approaches are made: a continuous-time and a discrete-time control. The proposed designs, continuous-time and discrete-time, are applied to the active suspension module simulator from Quanser. Results from computer simulations and experimental tests are analyzed to show the effectiveness of the proposed control strategy.

## 1. Introduction

There are different approaches to control active suspension systems: $H_\infty$ control [1, 2], proportional integral sliding mode control [3, 4], linear quadratic regulator [5], fuzzy controllers [6], artificial neural networks [7], and so forth. In this paper focus is given to problems that can arise when computers do the control. In this context, the sampling time involved in the process and possible delays sampled signals may damage the control performance. These signal delays can arise in Networked Control Systems (NCS) where the communication between the elements of the control loop is done by a nonideal shared digital network [8, 9]. Wireless Networked Control Systems (WNCS) usually show delays of many sampling periods and cannot be ignored [10].

The main advantage of Variable Structure Control with Sliding Mode (VSC/SM) is its robustness with respect to matched uncertainties, representing disturbances in control input, and parametric uncertainties or even system modeling uncertainties, provided that they belong to the image of the control input matrix [11, 12]. When the control signal is generated by microprocessors, besides sampling time, the system performance is greatly compromised when delays in both data acquisition and data transmission occur. In VSC/SM, this issue is even more important. By using a high speed switching control law in order to take the states trajectory to a sliding surface dependent on the current states, if the states used are delayed, the control law may not direct the states to this surface, which can also generate performance loss or even lead system to instability [13, 14]. The damage caused by delays to sliding mode control motivates several studies [15–18].

This paper proposes a strategy that uses state predictors along with VSC/SM in order to perform control of an active suspension system in presence of input control disturbance and data acquisition delay of many sampling periods. With purpose of comparison, it proposes two designs: one continuous-time control and one discrete-time control. In both cases, the control signal is generated from a digital computer.

For the purpose of illustration, the results from proposed controls, both continuous and discrete, are compared with the results of a linear quadratic regulator [19, 20] proposed by Quanser, the manufacturer of the active suspension system used in the practice tests.

## 2. Control Strategies Proposed

The objective of variable structure control with sliding mode, by means of a high speed switching control law, is to lead the state trajectory of the system to a surface in the state space and ensure that it holds to this surface. The surface is designed so that the system presents a desired dynamic when in sliding mode. Thus, the VSC/SM design is made up of two steps: the design of the switching surface and the design of the control law [12].

This section presents two controllers designs for state delayed systems: one uses continuous-time equations and the other uses discrete-time equations; that is, the sampling period of the computer is taken into account. In both projects, the proposed control strategy is to use a state predictor to estimate the current states, which forms the VSC/SM law. In this work the sampling period and the data acquisition delay are considered as known. Also, all the states of the plant are considered available.

*2.1. Design of Sliding Surface.* Consider a continuous-time system in the regular form given by (1), where $x_1(t) \in \mathfrak{R}^{n-m}$, $x_2(t) \in \mathfrak{R}^{m}$, $B \in \mathfrak{R}^{m\times m}$, $A_{11} \in \mathfrak{R}^{(n-m)\times(n-m)}$, $A_{12} \in \mathfrak{R}^{(n-m)\times m}$, $A_{21} \in \mathfrak{R}^{m\times(m-1)}$, and $A_{22} \in \mathfrak{R}^{m\times m}$ are constant matrices:

$$\begin{bmatrix} \dot{x}_1 \\ \dot{x}_2 \end{bmatrix} = \begin{bmatrix} A_{11} & A_{12} \\ A_{21} & A_{22} \end{bmatrix} \begin{bmatrix} x_1 \\ x_2 \end{bmatrix} + \begin{bmatrix} 0 \\ B \end{bmatrix} u(t). \tag{1}$$

The linear sliding surface proposed is given by (2), where $S_1 \in \mathfrak{R}^{m\times(n-m)}$, $S_2 \in \mathfrak{R}^{m\times m}$, and $\sigma(t) \in \mathfrak{R}^{m}$:

$$\sigma(t) = Sx(t) = \begin{bmatrix} S_1 & S_2 \end{bmatrix} \begin{bmatrix} x_1(t) \\ x_2(t) \end{bmatrix}. \tag{2}$$

Under these conditions, the dynamics of the states in sliding mode is described by (3) [12]. Note that the dynamics of the system, which previously had dimension $n$, is replaced by dimension $n-m$ when in sliding mode:

$$\dot{x}_1(t) = \left[A_{11} - A_{12}S_2^{-1}S_1\right] x_1(t). \tag{3}$$

The dynamics described by (3) has state feedback structure; thus one can use standard techniques to find the gain, as pole placement or quadratic optimal control [19].

Note that the sliding surface design in discrete-time is made in an analogous manner to the continuous-time one, and when the original system is not in the regular form, a nonsingular coordinate transformation can be used to put it in this form [21].

*2.2. Continuous-Time Control Design.* Consider the following system:

$$\dot{x}(t) = Ax(t) + Bu(t), \tag{4}$$

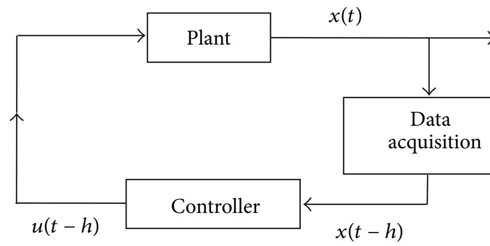


Figure 1: Representation of data acquisition delay using emulation.

where $x(t) \in \mathfrak{R}^{n}$ is the state vector; $u(t) \in \mathfrak{R}^{m}$ is the control vector; the matrices $A$ and $B$ are constants and with appropriate dimensions.

In this paper, it is considered that the control signals are generated by microprocessor and the states feedback is done by a data acquisition system, including analog/digital converters. Time delays may occur in data acquisition and data transmission; these delays are considered known and constant. Figure 1 is a schematic in which is illustrated this condition through emulation, that is, using small sampling periods so that the system can be approximated as a continuous-time.

If the control signals are generated from the delayed-time sampled states $x(t-h)$, then the controller will generate the control signal $u(t-h)$; that is, controlled plant (4) that was free of delay becomes a plant with delay described by (5):

$$\dot{x}(t-h) = Ax(t-h) + Bu(t-h). \tag{5}$$

Generally delays adversely affect the performance of control systems, whatever control method is used. In particular, under the approach of the VSC/SM, eliminating the data acquisition delay becomes important, because it is very sensitive to any kind of delay.

The estimator presented in (6) [22] will be used in order to estimate the current state:

$$x_p(t) = e^{Ah}x(t-h) + \int_{-h}^{0} e^{-A\theta}Bu(t+\theta)\,d\theta, \tag{6}$$

where $x_p(t)$ is the estimate of the current state vector ($x(t-h+h) = x(t)$).

The dynamics of the predictive state vector $x_p(t)$ is free of delay as can be viewed by (8), from the time derivative of $x_p(t)$, as follows:

$$\begin{aligned} \dot{x}_p(t) &= e^{Ah}\dot{x}(t-h) + Bu(t) - e^{Ah}Bu(t-h) \\ &\quad + A\int_{-h}^{0} e^{-A\theta}Bu(t+\theta)\,d\theta. \end{aligned} \tag{7}$$

Substituting (5) into (7), one has

$$\begin{aligned}\dot{x}_p(t) &= e^{Ah}Ax(t-h) + e^{Ah}Bu(t-h) + Bu(t) \\ &\quad - e^{Ah}Bu(t-h) + A\int_{-h}^{0} e^{-A\theta}Bu(t+\theta)\,\mathrm{d}\theta \\ &= A\left\{\underbrace{e^{Ah}x(t-h) + \int_{-h}^{0} e^{-A\theta}Bu(t+\theta)\,\mathrm{d}\theta}_{x_p(t)}\right\} + Bu(t) \\ &= Ax_p(t) + Bu(t),\end{aligned} \tag{8}$$

that shows that the state predictive dynamics is free of delay.

Now, consider an uncertain system undergoes delay during data acquisition; in this case the dynamics of the system is represented by

$$\dot{x}(t-h) = Ax(t-h) + Bu(t-h) + \Delta f(t). \tag{9}$$

Applying the continuous predictor proposed, one has the following predictive state:

$$x_p(t) = e^{Ah}x(t-h) + \int_{-h}^{0} e^{-A\theta}Bu(t+\theta)\,\mathrm{d}\theta. \tag{10}$$

Again, its dynamics are calculated as

$$\begin{aligned}\dot{x}_p(t) &= e^{Ah}\dot{x}(t-h) + A\int_{-h}^{0} e^{-A\theta}Bu(t+\theta)\,\mathrm{d}\theta \\ &\quad + Bu(t) - e^{Ah}Bu(t-h).\end{aligned} \tag{11}$$

But replacing (9) in (11)

$$\begin{aligned}\dot{x}_p(t) &= Ae^{Ah}x(t-h) + e^{Ah}Bu(t-h) + e^{Ah}\Delta f(t) \\ &\quad + A\int_{-h}^{0} e^{-A\theta}Bu(t+\theta)\,\mathrm{d}\theta + Bu(t) - e^{Ah}Bu(t-h) \\ &= A\left\{\underbrace{e^{Ah}x(t-h) + \int_{-h}^{0} e^{-A\theta}Bu(t+\theta)\,\mathrm{d}\theta}_{x_p(t)}\right\} \\ &\quad + Bu(t) + e^{Ah}\Delta f(t) \\ &= Ax_p(t) + Bu(t) + e^{Ah}\Delta f(t).\end{aligned} \tag{12}$$

Therefore, in this case, the initial uncertainty of the system $\Delta f(t)$ becomes $e^{Ah}\Delta f(t)$ and may influence the system dynamics in sliding even though it was originally a matched uncertainty. Thus, even when the system presents uncertainties in the plant, the dynamics of predictive state remain free of delays.

Therewith, one can develop the conventional VSC/SM design from predictive state vector $x_p(t)$. The sliding surface is given by

$$\sigma(t) = Sx_p(t), \tag{13}$$

where $S \in \mathfrak{R}^{m\times n}$ is one constant matrix, which establishes the system dynamics in sliding mode.

The purpose of the VSC/SM is to find a control law which ensures the existence of the sliding mode. A control law that achieves this goal consists of one continuous part along with one discontinuous part, as proposed in Decarlo et al. [12]:

$$u(t) = u_{\mathrm{eq}}(t) + u_N(t), \tag{14}$$

where $u_{\mathrm{eq}}(t)$ is the continuous part called equivalent control and $u_N(t)$ is the discontinuous part.

The equivalent control is that which determines the dynamics of the system in sliding mode. It is found using the condition described by

$$\dot{\sigma}(t) = S\dot{x}_p(t) = 0. \tag{15}$$

Given that in sliding mode $u_N(t) = 0$ and considering the product $SB$ nonsingular, we have

$$\dot{\sigma}(t) = S\left(Ax_p(t) + Bu_{\mathrm{eq}}(t)\right) = 0, \tag{16}$$

$$u_{\mathrm{eq}}(t) = -(SB)^{-1}(SA)\,x_p(t). \tag{17}$$

The discontinuous control part ($u_N(t)$) is responsible for bringing and maintaining the system state trajectory to the sliding surface. It is found using a generalized Lyapunov function which ensures the convergence of state trajectory to the sliding surface. Consider the following Lyapunov function candidate:

$$V(t) = \frac{1}{2}\sigma(t)^T\sigma(t). \tag{18}$$

The time derivative of $V(t)$ is negative definite if

$$\dot{V}(t) = \sigma(t)^T\dot{\sigma}(t) < 0. \tag{19}$$

In view of the control given in (14) and (17) it follows that

$$\dot{\sigma}(t) = (SB)\,u_N(t). \tag{20}$$

A control law that satisfies (19) considering (20) and assuming $SB = I$ is given in

$$u_N(t) = \left[u_{N1}(t) \ \cdots \ u_{Nm}(t)\right]^T, \tag{21}$$

where $u_{Ni}(t)$ is given by

$$u_{Ni}(t) = \rho_i\frac{\sigma_i(t)}{\left|\sigma_i(t)\right|}, \quad \rho_i < 0,\ i = 1,\dots,m. \tag{22}$$

Control law (22) suffers from the chattering problem. A modification to reduce this effect is proposed in Spurgeon and Davies [23] and presented in

$$u_{Ni}(t) = \rho_i\frac{\sigma_i(t)}{\left|\sigma_i(t)\right| + \delta_i}, \quad \rho_i < 0,\ \delta_i \longrightarrow 0^+,\ i = 1,\dots,m. \tag{23}$$

This paper will use only the expression continuous sliding mode control (CSMC) to refer to the control described by (14), (17), (21), and (23).

*2.3. Discrete-Time Control Design.* In the control scheme shown in Figure 1, it is assumed now that the signals are sampled in the sampling period $Ta$. Thus, the dynamic representation of the controlled plant in discrete-time state space is given by

$$x(k+1) = \Phi x(k) + \Gamma v(k), \tag{24}$$

where $x(k)$ is the state vector sampled at time $kTa$ and $v(k)$ is the control vector created at the same time. The matrices $\Phi \in \mathfrak{R}^{n\times n}$ and $\Gamma \in \mathfrak{R}^{n\times m}$ are constants and they depend on the sampling period $Ta$.

Now, the time delay in the system states caused by data acquisition and/or data transmission is taken into account. This delay is given by $h = HTa$. Similar to the continuous case, if the control signals are generated from the delayed sampled states $x(k-H)$ then the control law will be $v(k-H)$; that is, controlled plant (24), that was free of delay, becomes a plant with control delayed in $H$ samples. So the representation of the system dynamics sampled with delay is given by

$$x(k-H+1) = \Phi x(k-H) + \Gamma v(k-H). \tag{25}$$

In order to estimate the current states sampled, an estimator in the form of (26), adapted from Xia et al. [24], is used:

$$x_p(k) = \Phi^H x(k-H) + \sum_{i=-H+1}^{0} \Phi^{-i}\Gamma v(k-1+i), \tag{26}$$

where $x_p(k)$ is the current vector state estimate ($x(k-H+H) = x(k)$).

The dynamics of the predictive state is free of delay as can be seen from (28) by calculating $x_p(k+1)$, as follows:

$$x_p(k+1) = \Phi^H x(k-H+1) + \sum_{i=-H+1}^{0} \Phi^{-i}\Gamma v(k+i). \tag{27}$$

Substituting (25) into (27), it comes to

$$\begin{aligned}
x_p&(k+1)\\
&= \Phi^H [\Phi x(k-H) + \Gamma v(k-H)]\\
&\quad + \sum_{i=-H+1}^{0} \Phi^{-i}\Gamma v(k+i)\\
&= \Phi^H \Phi x(k-H) + \Phi^H \Gamma v(k-H)\\
&\quad + \sum_{i=-H+1}^{0} \Phi^{-i}\Gamma v(k+i)\\
&= \Phi^H \Phi x(k-H)\\
&\quad + \left[\sum_{i=-H+1}^{-1} \Phi^{-i}\Gamma v(k+i) + \Phi^H \Gamma v(k-H)\right] + \Gamma v(k)\\
&= \Phi\Phi^H x(k-H) + \sum_{i=-H}^{-1} \Phi^{-i}\Gamma v(k+i) + \Gamma v(k)\\
&= \Phi\Phi^H x(k-H) + \sum_{i=-H+1}^{0} \Phi^{-i+1}\Gamma v(k+i-1) + \Gamma v(k)\\
&= \Phi \left\{\underbrace{\Phi^H x(k-H) + \sum_{i=-H+1}^{0} \Phi^{-i}\Gamma v(k-1+i)}_{x_p(k)}\right\} + \Gamma v(k)\\
&= \Phi x_p(k) + \Gamma v(k).
\end{aligned} \tag{28}$$

If the digital system with data acquisition delay considered is uncertain, as described by (29)

$$x(k-H+1) = \Phi x(k-H) + \Gamma v(k-H) + \Delta f(k), \tag{29}$$

the predictive state is given by

$$x_p(k) = \Phi^H x(k-H) + \sum_{i=-H+1}^{0} \Phi^{-i}\Gamma v(k-1+i). \tag{30}$$

Calculating $x_p(k+1)$ it follows that

$$x_p(k+1) = \Phi^H x(k-H+1) + \sum_{i=-H+1}^{0} \Phi^{-i}\Gamma v(k+i). \tag{31}$$

Using (29) one reaches

$$\begin{aligned}
x_p(k+1) &= \Phi^H [\Phi x(k-H) + \Gamma v(k-H) + \Delta f(k)]\\
&\quad + \sum_{i=-H+1}^{0} \Phi^{-i}\Gamma v(k+i)\\
&= \Phi^{H+1} x(k-H) + \Phi^H \Gamma v(k-H)\\
&\quad + \Phi^H \Delta f(k) + \sum_{i=-H+1}^{0} \Phi^{-i}\Gamma v(k+i)\\
&= \Phi^{H+1} x(k-H) + \sum_{i=-H}^{-1} \Phi^{-i}\Gamma v(k+i)\\
&\quad + \Gamma v(k) + \Phi^H \Delta f(k)
\end{aligned}$$

$$
\begin{aligned}
&= \Phi^{H+1} x(k-H) + \sum_{i=-H+1}^{0} \Phi^{-i+1} \Gamma v(k+i-1) \\
&\quad + \Gamma v(k) + \Phi^{H} \Delta f(k) \\
&= \Phi \left[ \underbrace{\Phi^{H} x(k-H) + \sum_{i=-H+1}^{0} \Phi^{-i} \Gamma v(k+i-1)}_{x_p(k)} \right] \\
&\quad + \Gamma v(k) + \Phi^{H} \Delta f(k) \\
&= \Phi x_p(k) + \Gamma v(k) + \Phi^{H} \Delta f(k).
\end{aligned} \tag{32}
$$

Thus, the dynamics of predictive state is free from delays even in the presence of uncertainties in the plant. Note that $\Delta f(k)$ has been multiplied by $\Phi^H$; that is, assuming that $\Delta f(k)$ was initially a matched uncertainty it lets this condition bypass through the predictor.

Therefore, as the predictive state dynamics is free of delay one can develop the VSC/SM design from the predictive state vector $x_p(k)$. A discrete sliding surface is given by

$$\sigma(k) = G x_p(k), \tag{33}$$

where $G \in \Re^{m \times n}$ is a constant matrix, which establishes the system's dynamic in sliding mode.

The discrete control law that establishes a sliding mode is proposed by Garcia et al. [25]:

$$v(k) = v_{\text{eq}}(k) + v_N(k), \tag{34}$$

where $v_{\text{eq}}(k)$ is the equivalent control that determines the dynamics of the system in sliding mode and $v_N(k)$ is responsible for taking the system to the sliding mode.

The equivalent control is found when it is guaranteed that the state trajectory remains on the surface, that is,

$$\sigma(k+1) = G x_p(k+1) = \sigma(k) = G x_p(k). \tag{35}$$

Replacing the system (25) into (35), considering $G\Gamma$ nonsingular, and recalling that in sliding mode $v_N(k) = 0$, one finds

$$v_{\text{eq}}(k) = -(G\Gamma)^{-1} G (\Phi - I) x_p(k), \tag{36}$$

where $I$ denotes the identity matrix with appropriate dimensions.

The control $v_N(k)$ is chosen to ensure the convergence of the state trajectory to the sliding surface. This problem is similar to a stability problem, and one can use the discrete-time Lyapunov's second method to solve this.

Consider the following Lyapunov function candidate:

$$V(k) = \sigma(k)^T \sigma(k). \tag{37}$$

To ensure convergence $V(k+1) < V(k)$ must be true. Substituting (37) in this condition, one has

$$\sigma(k+1)^T \sigma(k+1) < \sigma(k)^T \sigma(k). \tag{38}$$

Note that

$$
\begin{aligned}
\Delta\sigma(k) &= \sigma(k+1) - \sigma(k) \\
&= G x_p(k+1) - G x_p(k) \\
&= G\left[\Phi x_p(k) + \Gamma v(k)\right] - G x_p(k).
\end{aligned} \tag{39}
$$

Considering (34) and (36), one comes to

$$\Delta\sigma(k) = G\Gamma v_N(k). \tag{40}$$

From (38) one has

$$\sigma(k)^T \Delta\sigma(k) < -\frac{1}{2} \Delta\sigma(k)^T \Delta\sigma(k). \tag{41}$$

Substituting (40) into (41)

$$\sigma(k)^T G\Gamma v_N(k) < -\frac{1}{2} \left[G\Gamma v_N(k)\right]^T \left[G\Gamma v_N(k)\right]. \tag{42}$$

Assuming $G\Gamma = I$, condition (42) becomes

$$\sigma(k)^T v_N(k) < -\frac{1}{2} v_N(k)^T v_N(k). \tag{43}$$

A control law that satisfies (43) is (44) along with (45):

$$v_N(k) = \left[v_{N1}(k) \ \cdots \ v_{Nm}(k)\right]^T, \tag{44}$$

$$v_{Ni}(k) = -\gamma_i \sigma_i(k), \quad 0 < \gamma_i < 2. \tag{45}$$

In this text only the expression discrete sliding mode control (DSMC) will be used to refer to control law (34), (36), and (44)-(45).

## 3. Application to Active Suspension System

*3.1. Mathematical Model.* There are three different active vehicle suspensions models found in the literature. These are entire vehicle suspension models [1, 7], half car models [3, 4], and quarter car models [2, 5, 6, 26].

This paper utilizes a state space linear model of a quarter of vehicle corresponding to Quanser's bench active suspension system. Its diagram is shown in Figure 2 [20].

The active suspension system can be modeled as a double mass-spring-damper system [20]. Thus, the two system inputs are control signal $F_c(t)$ and the derivative of road surface $\dot{z}_r(t)$.

The coordinate $z_{us}(t)$ represents the displacement of the tire, which has mass $M_{us}$, and the coordinate $z_s(t)$ represents the displacement of the vehicle body, which has mass $M_s$. The movements are related to the movement imposed by the road surface on which the vehicle is traveling $z_r(t)$.

The motion equations of the system are obtained using the free body diagram method and can be described in the state space in the form of (46). The Quanser Innovate Educate [20] presents a detailed deduction of this model:

$$\dot{x}(t) = A x(t) + B_1 e(t) + B_2 u(t). \tag{46}$$

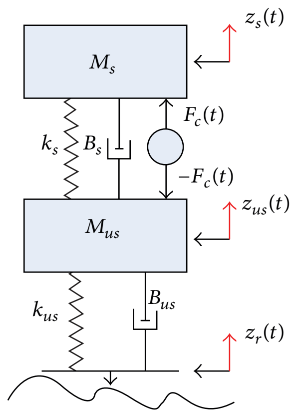


FIGURE 2: Diagram of Quanser's bench active suspension system [20].

In (46), the $B_1$ is the related matrix to the road surface derivative ($\dot{z}_r(t)$) and $B_2$ is the related matrix to the control signal ($F_c(t)$).

The four states considered accessible are defined in

$$x(t) = \begin{bmatrix} z_s(t) - z_{us}(t) \\ \dot{z}_s(t) \\ z_{us}(t) - z_r(t) \\ \dot{z}_{us}(t) \end{bmatrix}. \tag{47}$$

The first state is the suspension travel. The second state is the vehicle body vertical velocity. The third state is the tire deflection. The fourth state is the wheel vertical velocity. The first input, $e(t)$, is the road surface velocity ($\dot{z}_r(t)$). The second input, $u(t)$, is the control action ($F_c(t)$).

The matrices $A$, $B_1$, and $B_2$ from (46) are shown in

$$A = \begin{bmatrix} 0 & 1 & 0 & -1 \\ -\frac{k_s}{B_s} & -\frac{B_s}{M_s} & 0 & -\frac{B_s}{M_s} \\ 0 & 0 & 0 & 1 \\ \frac{k_s}{M_{us}} & \frac{B_s}{M_{us}} & -\frac{k_{us}}{M_{us}} & -\frac{B_s + B_{us}}{M_{us}} \end{bmatrix},$$
$$B_1 = \begin{bmatrix} 0 \\ 0 \\ -1 \\ \frac{B_{us}}{M_{us}} \end{bmatrix}, \qquad B_2 = \begin{bmatrix} 0 \\ \frac{1}{M_s} \\ 0 \\ -\frac{1}{M_{us}} \end{bmatrix}. \tag{48}$$

*3.2. Application of the Proposed Control to Active Suspension with Data Acquisition Delay.* The numerical values of the state space matrices $A$, $B_1$, and $B_2$, in (46) and (48), are calculated from data provided by the manufacturer's manual [27], shown in Table 1.

The calculations involved in the design of the controllers were performed using Matlab language and based on the nominal values given by the manufacturer. However, in Section 4 uncertainties were included in order to demonstrate robustness, shown in Section 2.

TABLE 1: Physical parameters of Quanser's bench active suspension system [27].

| Description | Symbol | Value |
|---|---|---|
| Spring stiffness between car body and tire | $k_s$ | 900 N/m |
| Damping coefficient between car body and tire | $B_s$ | 7,5 (N/m) $s$ |
| Car body mass | $M_s$ | 2,45 kg |
| Spring stiffness between tire and road | $k_{us}$ | 2500 N/m |
| Damping coefficient between tire and road | $B_{us}$ | 5 (N/m) $s$ |
| Tire mass | $M_{us}$ | 1 kg |

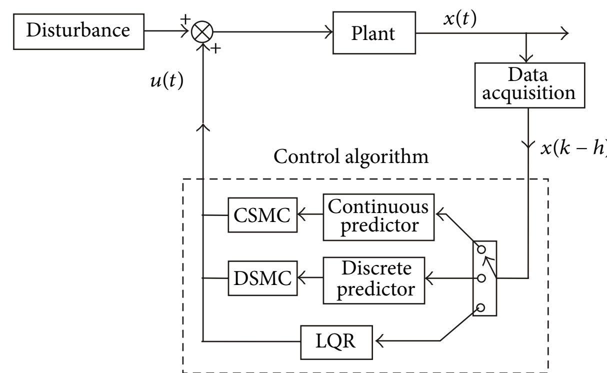


FIGURE 3: Comparison scheme between control methods.

For the continuous-time control design, (14), (17), (21), and (23), the $S$ matrix from sliding surface (13) was calculated as

$$S = \begin{bmatrix} 27.3055 & 2.2188 & -28.2237 & -0.0944 \end{bmatrix}. \tag{49}$$

Such poles on sliding mode are $p_1 = -23.0114$, $p_2 = -24.0955 + 25.1044j$, and $p_3 = -24.0955 - 25.1044j$. The other parameters used are $\rho = -25$ and $\delta = 0.06$, which were chosen empirically respecting the physical constraints imposed by the equipment. The sampling period for this control was chosen to be 1 ms so that the emulation presented good results.

For the discrete-time control design, (34), (36), and (44)-(45), it was considered 3 ms sampling period, and $G$ from (33) was designed as (50) such that the system poles in sliding mode in $z$ plane were $z_1 = 0.9333$, $z_2 = 0.9276 + 0.0700j$, and $z_3 = 0.9276 - 0.0700j$, corresponding to the poles chosen in continuous-time using the sample period established. It also used $\gamma = 0.3$, observing the equipment's restrictions:

$$G = \begin{bmatrix} 8397.4 & 682.9 & -8704.2 & -30.1 \end{bmatrix}. \tag{50}$$

In computer simulations, and also on the bench, it was implemented a scheme to compare the performances of CSMC and DSMC proposed in this paper and also a conventional LQR control proposed by the manufacturer [20]. Such scheme is shown in Figure 3 and has been implemented in Matlab/Simulink. The considered LQR

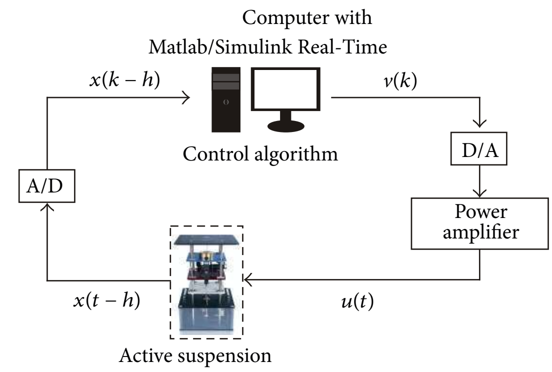


(a) Schematic

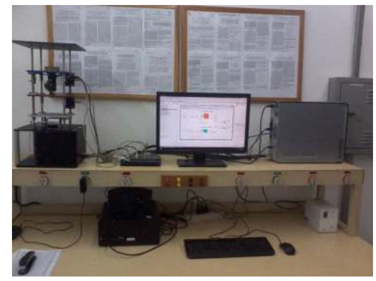

(b) Equipment

FIGURE 4: Experimental tests.

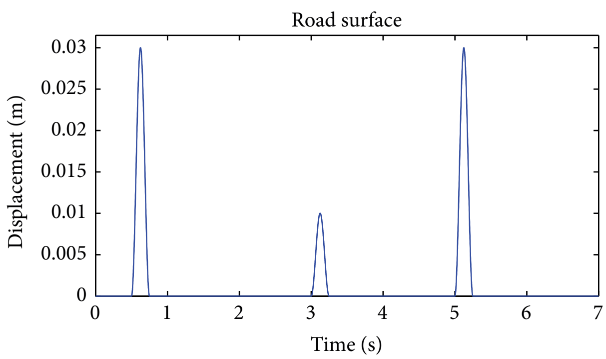


FIGURE 5: Road surface profile used [3, 4].

control minimizes the quadratic performance index $J = \int_0^\infty x(t)^T Q x(t) + u(t)^T R u(t) dt$ in continuous-time [19] or $J = \sum_0^\infty x(k)^T Q x(k) + v(k)^T R v(k)$ in discrete-time [28] and has as design matrices $Q = \text{diag}([450 \quad 30 \quad 5 \quad 0.01])$ and $R = 0.01$. Several other methods considered robust could be applied [1, 2, 7, 26].

The practical experiments were performed in Quanser's bench active suspension system [27] using Quanser's AMPAQ current amplifier [29] and QPID data acquisition board [30], according to the scheme shown in Figure 4(a). In this scheme, the computer (PC Dell with Intel Core Quad 2.40 GHz), provided with Matlab/Simulink Real-Time and Quanser Quarq v 2.2, implements the controls used: continuous-time and discrete-time LQR, continuous-time predictor CSMC and discrete-time predictor DSMC. Analog-to-digital converters are used in communication with the bench system. The equipment used in the experiments is presented in Figure 4(b), realizing that the equipment remains fixed on a bench, and the road surface is emulated by the movement of the lower plate of the equipment [20].

The format of the road surface was chosen based on the work of Sam and Osman [3] and Sam et al. [4], which represent a typical road surface by (51). It used $a = 0.03$ m for $0.5 \leq t \leq 0.75$ and $5 \leq t \leq 5.25$ and $a = 0.01$ m for $3 \leq t \leq 3.25$. In Figure 5 is presented the road surface profile used:

$$z_r(t) = \begin{cases} \dfrac{a(1-\cos(8\pi t))}{2} & \text{if } 0.5 \leq t \leq 0.75 \\ & \text{or } 3 \leq t \leq 3.25 \\ & \text{or } 5 \leq t \leq 5.25, \\ 0 & \text{otherwise.} \end{cases} \quad (51)$$

However, other road surfaces possibilities exist in the literature and could have been used like square wave [26] and random road profile [6, 7], among others [1, 5].

To check the robustness of the CSMD and DSMD controls, a disturbance in the control signal actuator was introduced in most tests. The disturbance used was a sine wave with frequency 0.2 Hz and amplitude equal to 4 N.

## 4. Obtained Results and Discussion

*4.1. Predictor Necessity.* In Figures 6 and 7 are presented simulation results for the CSMC and DSMC controls with sampling periods of 1 ms and 3 ms, respectively, and with a delay of 12 sample periods (12 ms and 36 ms) without predictors. As shown in these figures, data acquisition delays let CSMC and DSMC controls be ineffective.

In the Sections 4.2 and 4.3 is shown in simulation and practical experiments that the use of state predictors is effective means that enable use of variable structure control when there is data acquisition delay.

*4.2. Continuous-Time Control Results.* In Figures 8 and 9 is shown the response of the control system using CSMC with continuous predictor (CP-CSMC) compared with the LQR controller results, proposed by the manufacturer. In these graphs the system suffers delay of 12 sampling periods (12 ms) and disturbances in the control input. These graphs contain simulation and experimental results (using Quanser's bench active suspension system) on which one notes that the CP-CSMC rejected the disturbance.

In Figures 10 and 11 the results obtained when the data acquisition suffers 60 sampling periods' delay (60 ms) are

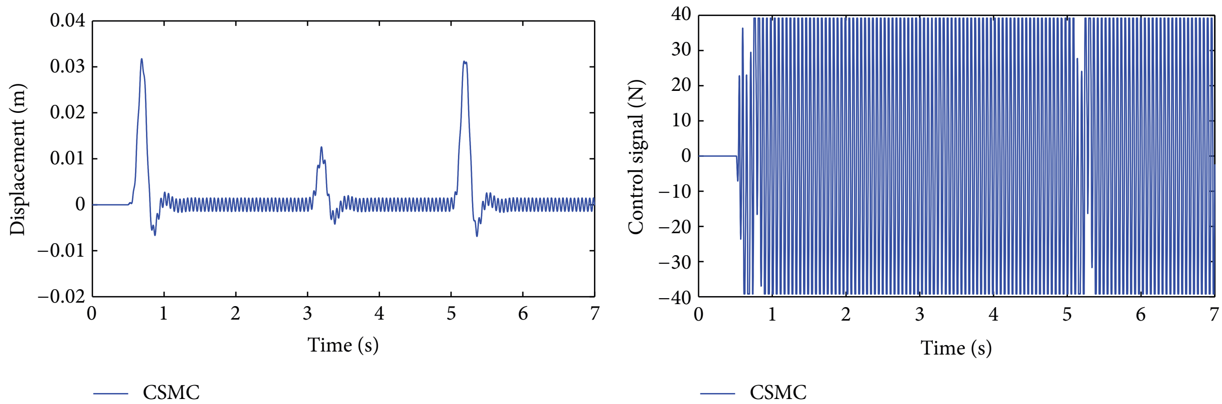


(a) Displacement simulation (b) Control signal simulation

Figure 6: Simulation results for CSMC control with 12 sampling periods' delay without predictor. (a) Car body displacement and (b) control signal.

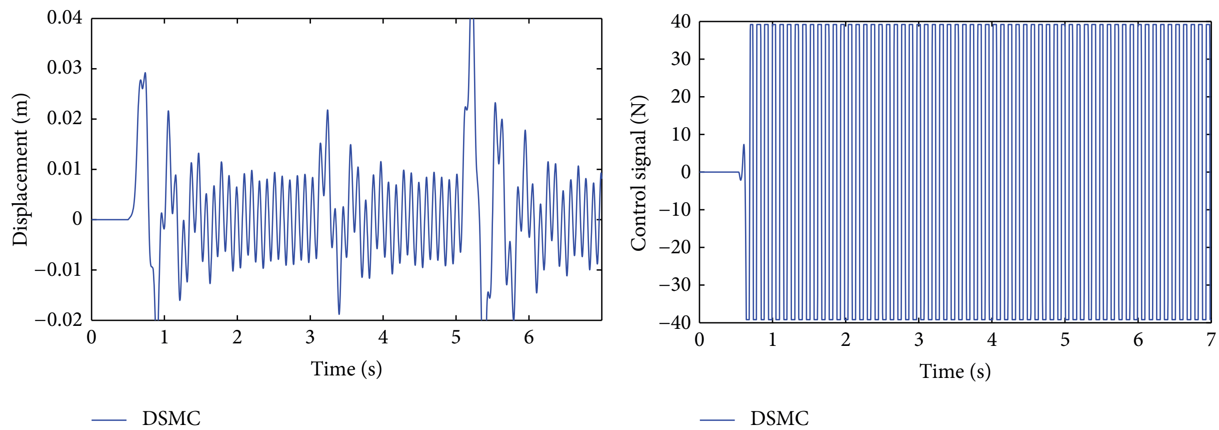


(a) Displacement simulation (b) Control signal simulation

Figure 7: Simulation results for DSMC control with 12 sampling periods' delay without predictor. (a) Car body displacement and (b) control signal.

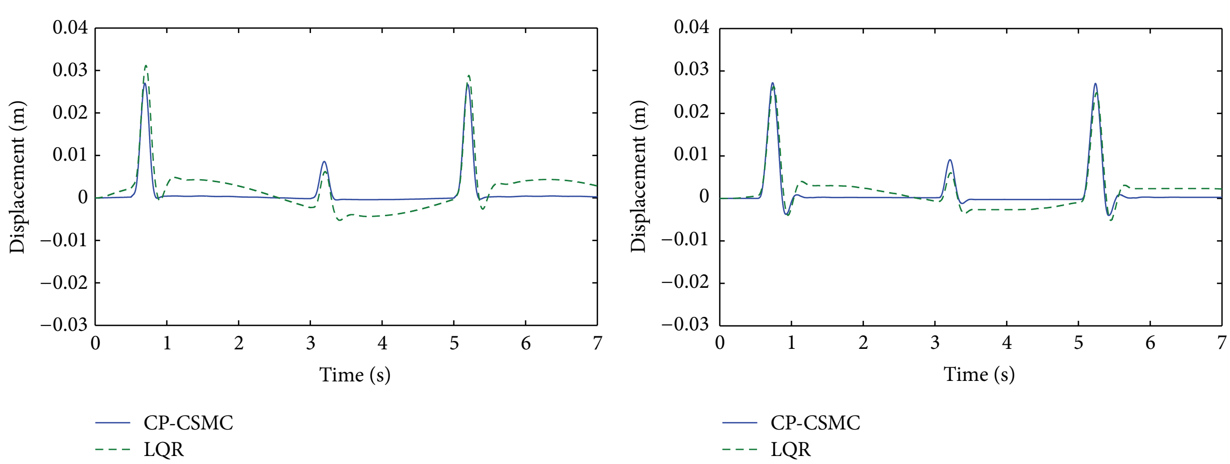


(a) Simulation result (b) Bench result

Figure 8: Car body displacement with delay of 12 sampling periods in data acquisition and disturbance in the control input.

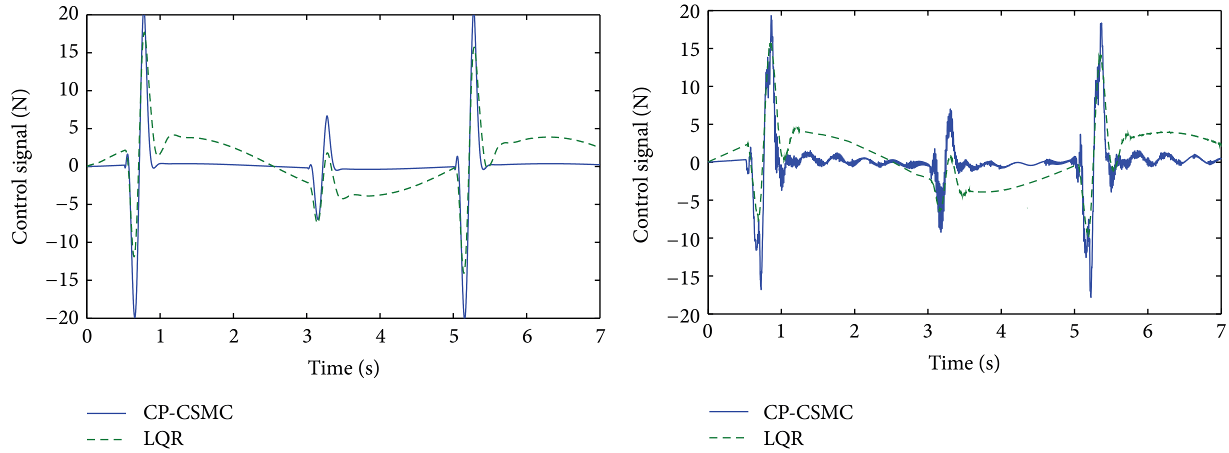


(a) Simulation result (b) Bench result

Figure 9: Control signal with delay of 12 sampling periods in data acquisition and disturbance in the control input.

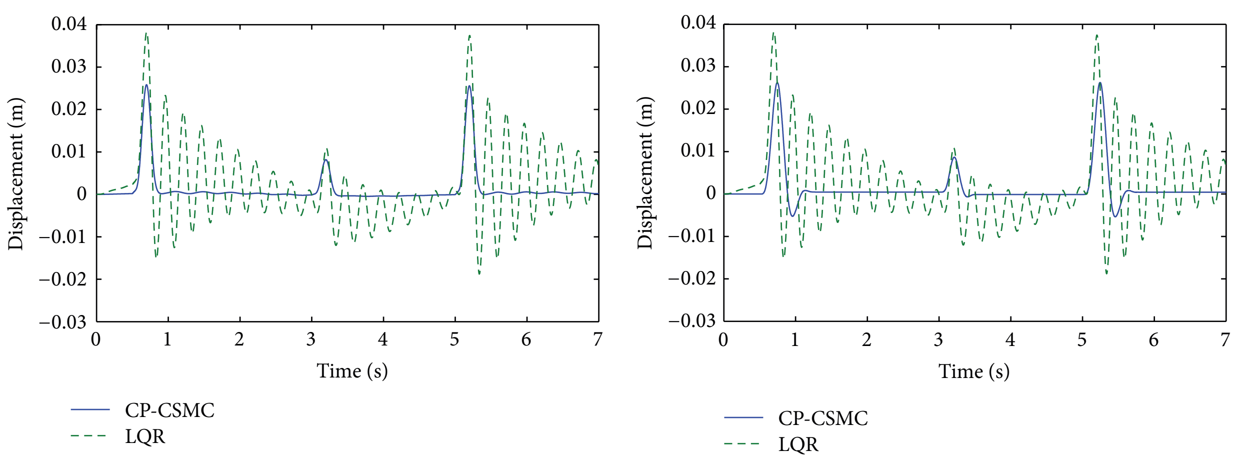


(a) Simulation result (b) Bench result

Figure 10: Car body displacement with delay of 60 sampling periods in data acquisition and disturbance in the control input.

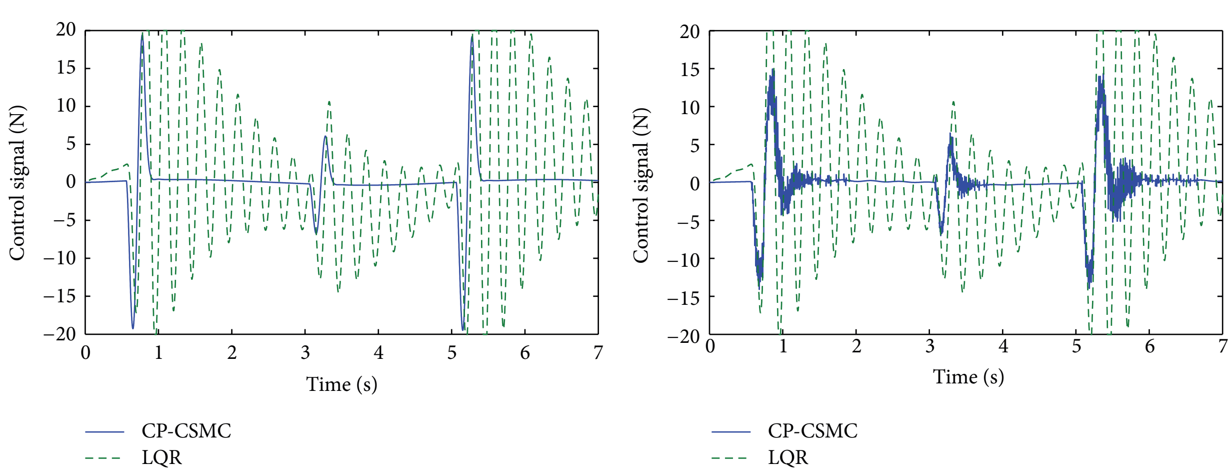


(a) Simulation result (b) Bench result

Figure 11: Control signal with delay of 60 sampling periods in data acquisition and disturbance in the control input.

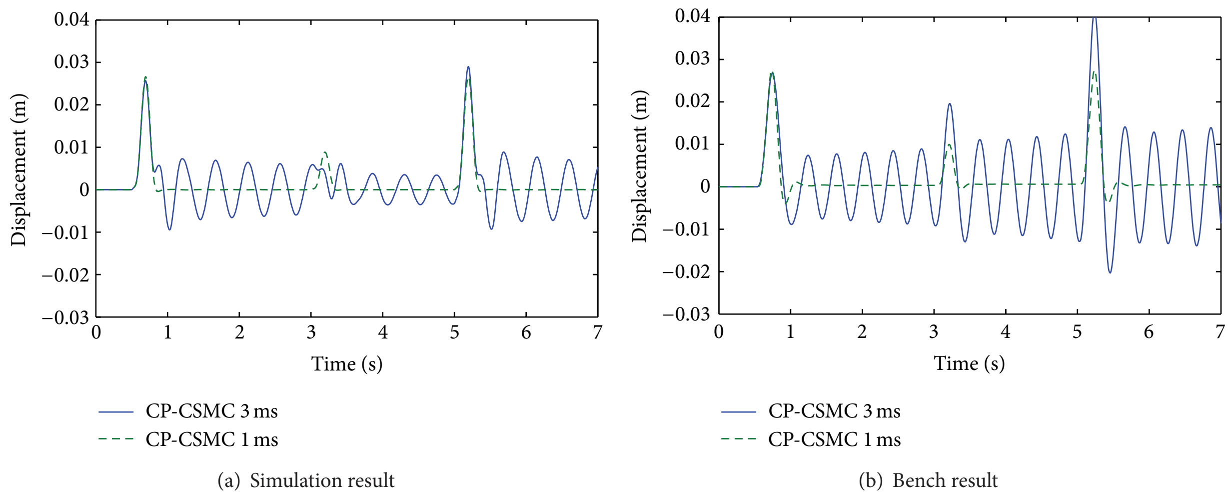


FIGURE 12: Comparison between car body displacements with delay of 12 sampling periods in data acquisition without disturbance in the control input using different sampling periods.

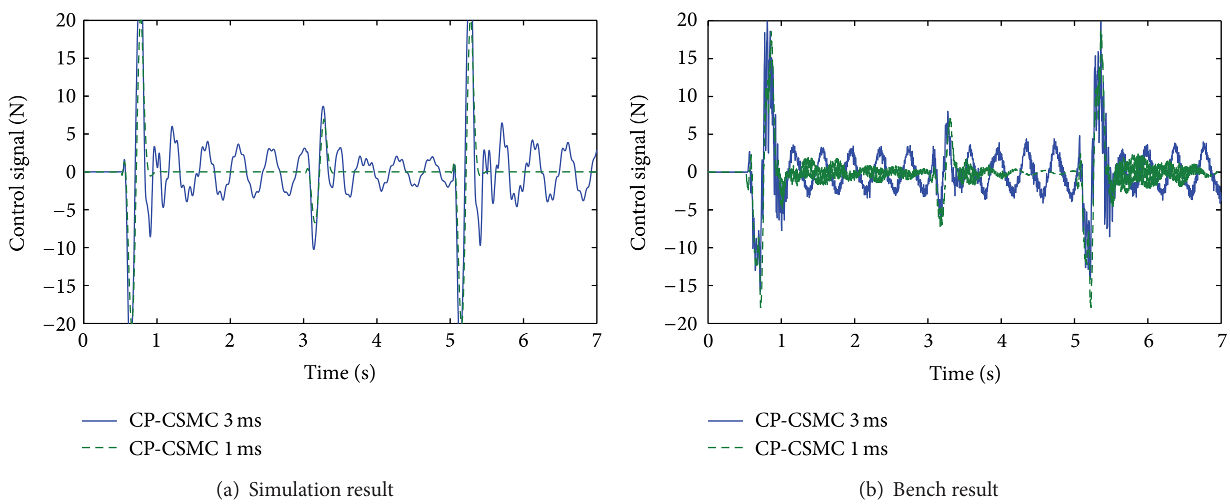


FIGURE 13: Comparison between control signals with delay of 12 sampling periods in data acquisition without disturbance in the control input using different sampling periods.

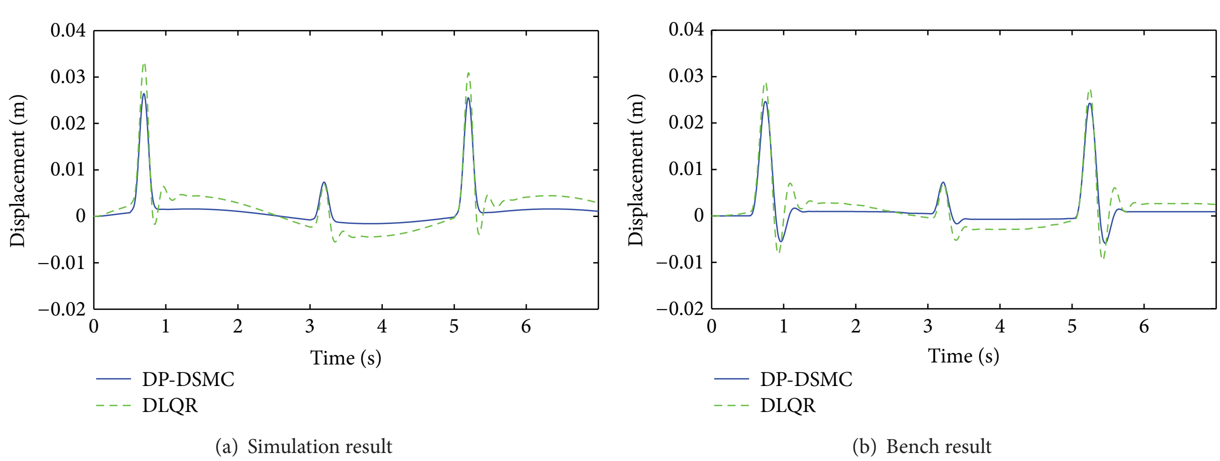


FIGURE 14: Car body displacement with delay of 12 sampling periods in data acquisition and disturbance in the control input.

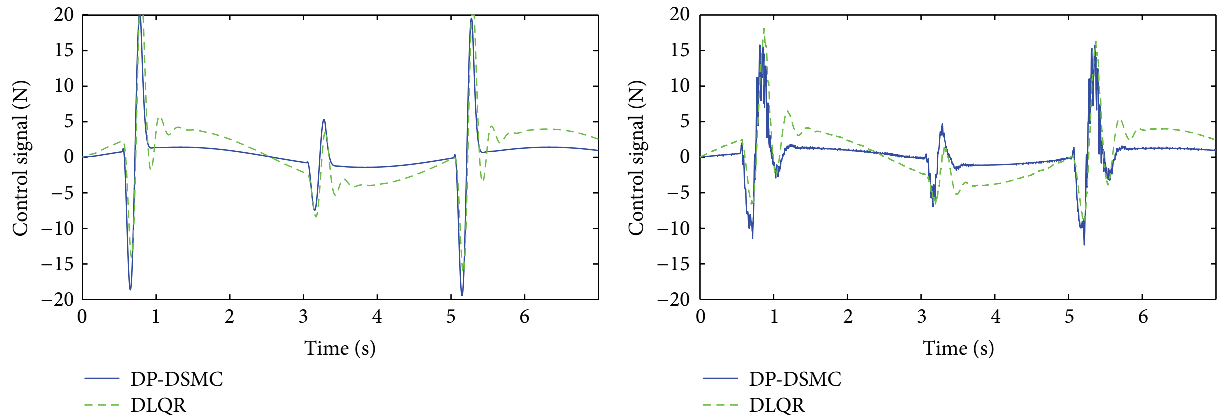


(a) Simulation result (b) Bench result

FIGURE 15: Control signal with delay of 12 sampling periods in data acquisition and disturbance in the control input.

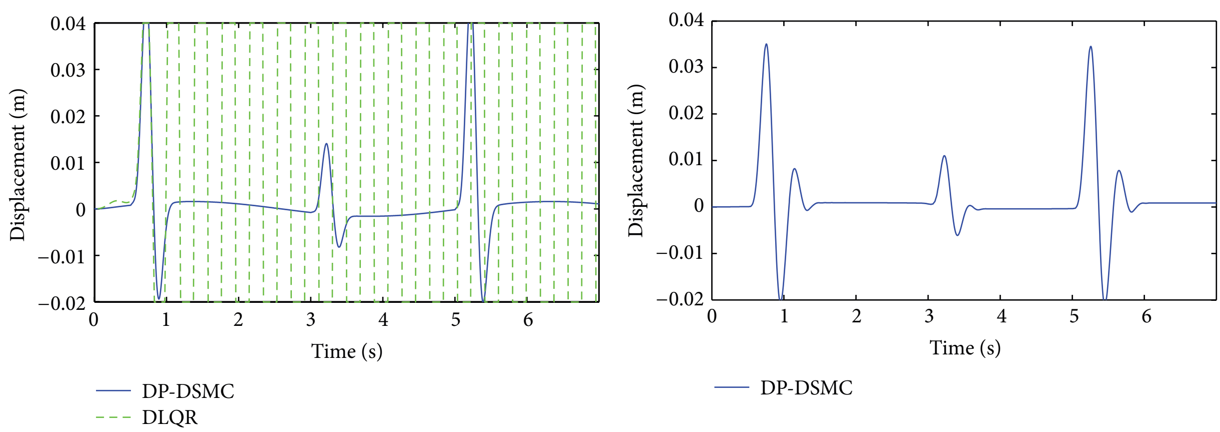


(a) Simulation result (b) Bench result

FIGURE 16: Car body displacement with delay of 60 sampling periods in data acquisition and disturbance in the control input.

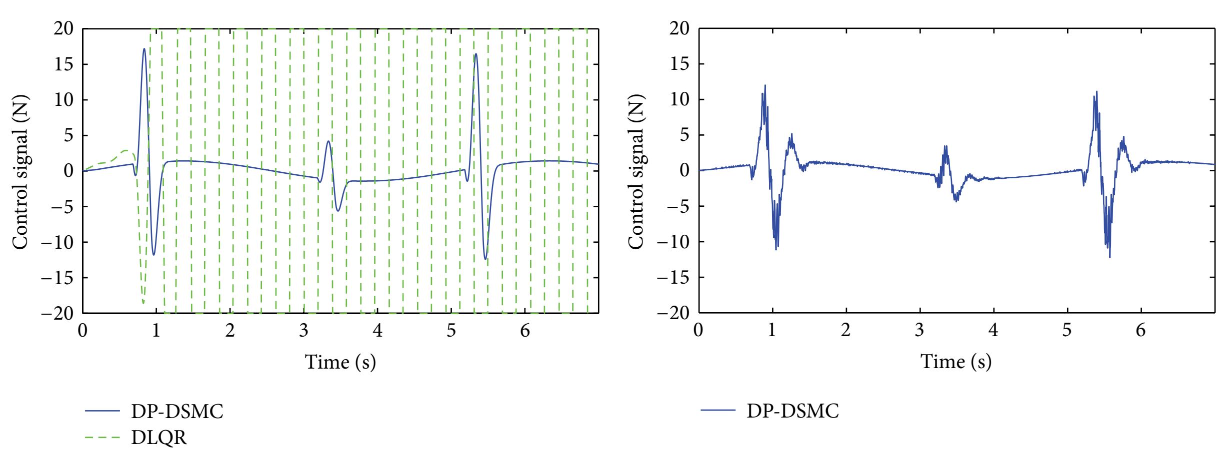


(a) Simulation result (b) Bench result

FIGURE 17: Control signal with delay of 60 sampling periods in data acquisition and disturbance in the control input.

shown. Even in this extreme condition, the control model composed of the pair continuous predictor-CSMC remained with good performance, while the LQR control showed very bad performance.

The graphs in Figures 8–11 demonstrate the effectiveness of continuous predictor along with CSMC to control systems with data acquisition delay when are used small sampling periods.

When this sampling period increases, the continuous control displays deterioration in their performance. It is no different from the proposed control, as can be seen in Figures 12 and 13 where, even in the absence of disturbance in the control input, the control performance of continuous predictor-CSMC is unsatisfactory when the sampling period is 3 ms.

To deal with larger sampling periods, where the emulation becomes inefficient, one uses the discrete control approach, whose results are presented in Section 4.3.

*4.3. Discrete-Time Control Results.* This test stage uses sampling periods of 3 ms, during which continuous control showed poor results. In Figures 14, 15, 16, and 17 are presented simulation and bench results to delays in data acquisition from 12 and 60 sampling periods (36 ms and 180 ms) and disturbance in the control input of the system with discrete predictor-DSMC (DP-DSMC). The results are compared with the discrete LQR results (DLQR) designed with matrices proposed by Quanser, the manufacturer of the active suspension system bench.

Note that the pair discrete predictor-DSMC remained with good results even when the system suffers large delays in data acquisition and the LQR controller, despite its lower sensitivity to such delays, cannot resist the delay of 60 sampling periods of delay, and bench results were not possible in this case.

## 5. Conclusions

In this paper, the problem of data acquisition delays in continuous-time and discrete-time sliding mode control when performed by a computer was analyzed.

An approach containing a state predictor has been successfully employed in order to overcome the problem of data acquisition delay, even in the presence of large delays, along with either continuous or discrete sliding mode control.

In the absence of state predictor, it was shown that controls CSMC and DSMC have poor results when there is data acquisition delay in the system. Moreover, it was shown that the use of predictors is able to overcome this difficulty, in simulations and practical applications. So the CP-CSMC and DP-DSMC controllers reject the matched uncertainty, even with delay time presence.

## Conflict of Interests

The authors declare that there is no conflict of interests regarding the publication of this paper.

## Acknowledgments

The authors thank the Coordination of Improvement of Higher Education Personnel (CAPES) for financial support and FAPESP (Process no. 2011/17610-0) for the acquisition of the active suspension system.

## References

[1] M. Yamashita, K. Fujimori, K. Hayakawa, and H. Kimura, “Application of $H_\infty$ control to active suspension systems,” *Automatica*, vol. 30, no. 11, pp. 1717–1729, 1994.

[2] C. Lauwerys, J. Swevers, and P. Sas, “Robust linear control of an active suspension on a quarter car test-rig,” *Control Engineering Practice*, vol. 13, no. 5, pp. 577–586, 2005.

[3] Y. M. Sam and J. H. S. B. Osman, “Modeling and control of the active suspension system using proportional integral sliding mode approach,” *Asian Journal of Control*, vol. 7, no. 2, pp. 91–98, 2005.

[4] Y. M. Sam, N. M. Suaib, and J. H. S. Osman, “Proportional integral sliding mode control for the half-car active suspension system with hydraulic actuator,” in *Proceedings of the 8th WSEAS International Conference on Robotics, Control and Manufacturing Technology (ROCOM ’08)*, pp. 52–57, Hangzhou, China, 2008.

[5] M. Nagarkar, G. Vikhe, K. Borole, and V. Nandedkar, “Active control of quarter-car suspension system using linear quadratic regulator,” *International Journal of Automotive and Mechanical Engineering*, vol. 3, pp. 364–372, 2011.

[6] C.-S. Ting, T.-H. S. Li, and F.-C. Kung, “Design of fuzzy controller for active suspension system,” *Mechatronics*, vol. 5, no. 4, pp. 365–383, 1995.

[7] İ. Eski and Ş. Yıldırım, “Vibration control of vehicle active suspension system using a new robust neural network control system,” *Simulation Modelling Practice and Theory*, vol. 17, no. 5, pp. 778–793, 2009.

[8] J. P. Hespanha, P. Naghshtabrizi, and Y. Xu, “A survey of recent results in networked control systems,” *Proceedings of the IEEE*, vol. 95, no. 1, pp. 138–162, 2007.

[9] L. Zhang, H. Gao, and O. Kaynak, “Network-induced constraints in networked control systems—a survey,” *IEEE Transactions on Industrial Informatics*, vol. 9, no. 1, pp. 403–416, 2013.

[10] M. Guinaldo, J. Sánchez, and S. Dormido, “Co-design strategy of networked control systems for treacherous network conditions,” *IET Control Theory and Applications*, vol. 5, no. 16, pp. 1906–1915, 2011.

[11] B. Draženović, “The invariance conditions in variable structure systems,” *Automatica*, vol. 5, no. 3, pp. 287–295, 1969.

[12] R. A. Decarlo, S. H. Zak, and G. P. Matthews, “Variable structure control of nonlinear multivariable systems: a tutorial,” *Proceedings of the IEEE*, vol. 76, no. 3, pp. 212–232, 1988.

[13] M. Dambrine, F. Gouaisbaut, W. Perruquetti, and J. P. Richard, “Robustness of sliding mode control under delays effects: a case study,” in *Proceedings of the 2nd IEEE-IMACS Conference on Computational Engineering in Systems Applications (CESA ’98)*, pp. 817–821, 1998.

[14] S. M. Lee and B. H. Lee, “A discrete-time sliding mode controller and observer with computation time delay,” *Control Engineering Practice*, vol. 7, no. 8, pp. 943–955, 1999.

[15] F. Gouaisbaut, M. Dambrine, and J. P. Richard, “Sliding mode control of linear time delay systems: a design via LMIs,” *Journal*

*of Mathematical Control and Information*, vol. 19, no. 1-2, pp. 83–94, 2002.

[16] F. Gouaisbaut, Y. Blanco, and J. P. Richard, "Robust sliding mode control of non-linear systems with delay: a design via polytopic formulation," *International Journal of Control*, vol. 77, no. 2, pp. 206–215, 2004.

[17] X. Han, E. Fridman, and S. K. Spurgeon, "Sliding-mode control of uncertain systems in the presence of unmatched disturbances with applications," *International Journal of Control*, vol. 83, no. 12, pp. 2413–2426, 2010.

[18] X. Han, E. Fridman, and S. K. Spurgeon, "Sliding mode control in the presence of input delay: a singular perturbation approach," *Automatica*, vol. 48, no. 8, pp. 1904–1912, 2012.

[19] K. Ogata, *Modern Control Engineering*, Instrumentation and Controls Series, Prentice Hall, Upper Saddle River, NJ, USA, 5th edition, 2010.

[20] "Active suspension LQG control using Quarc—instructor manual," Quanser Innovate Educate, 2010.

[21] A. G. Lukyanov and V. I. Utkin, "Methods of reducing equations for dynamic systems to a regular form," *Automation and Remote Control*, vol. 42, no. 4, pp. 413–420, 1981.

[22] T. Furukawa and E. Shimemura, "Predictive control for systems with time delay," *International Journal of Control*, vol. 37, no. 2, pp. 399–412, 1983.

[23] S. K. Spurgeon and R. Davies, "A nonlinear control strategy for robust sliding mode performance in the presence of unmatched uncertainty," *International Journal of Control*, vol. 57, no. 5, pp. 1107–1123, 1993.

[24] Y. Xia, G. P. Liu, P. Shi, J. Chen, D. Rees, and J. Liang, "Sliding mode control of uncertain linear discrete time systems with input delay," *IET Control Theory and Applications*, vol. 1, no. 4, pp. 1169–1175, 2007.

[25] J. Garcia, J. Ribeiro, J. Silva, and E. Martins, "Continuous-time and discrete-time sliding mode control accomplished using a computer," *IEE Proceedings—Control Theory and Applications*, vol. 152, no. 2, pp. 220–228, 2005.

[26] E. R. P. da Silva, E. Assuncao, M. C. Teixeira, and R. Cardim, "Robust controller implementation via state-derivative feedback in an active suspension system subjected to fault," in *Proceedings of the Conference on Control and Fault-Tolerant Systems (SysTol '13)*, pp. 752–757, 2013.

[27] "Active suspension system—user manual," Quanser Innovate Educate, 2010.

[28] G. F. Franklin, J. D. Powell, and M. L. Workman, *Digital Control of Dynamic Systems*, Addison-Wesley Longman, Menlo Park, Calif, USA, 3rd edition, 1998.

[29] "AMPAC—user manual," Quanser Innovate Educate, 2008.

[30] "QPID and QPIDe data acquisition boards—user manual," Quanser Innovate Educate, 2010.